

Supporting Information

A Luminescent G-quadruplex-Selective Iridium(III) Complex for the Label-Free Detection of Lysozyme

Lihua Lu,^{‡a} Wanhe Wang,^{‡a} Modi Wang,^{‡a} Tian-Shu Kang,^b Jin-Jian Lu,^b Xiu-Ping Chen,^b Quan-Bin Han,^c Chung-Hang Leung^b and Dik-Lung Ma^{*a}

^a *Department of Chemistry, Hong Kong Baptist University, Kowloon Tong, Hong Kong, China. *E-mail: edmondma@hkbu.edu.hk*

^b *State Key Laboratory of Quality Research in Chinese Medicine, Institute of Chinese Medical Sciences, University of Macau, Macao, China.*

^c *School of Chinese Medicine, Hong Kong Baptist University, 7 Baptist University Road, Kowloon Tong, Hong Kong*

[‡] *These authors contributed equally to this work.*

Chemicals and materials

Iridium chloride hydrate ($\text{IrCl}_3 \cdot x\text{H}_2\text{O}$) was purchased from Precious Metals Online (Australia). Other reagents were purchased from Sigma Aldrich (St. Louis, MO) and used as received. Lysozyme, bovine serum albumin (BSA), β -amyloid, ATP, thrombin, trypsin, and hemoglobin were also obtained from Sigma.

General experimental

Mass spectrometry was performed at the Mass Spectroscopy Unit at the Department of Chemistry, Hong Kong Baptist University, Hong Kong (China). Melting points were determined using a Gallenkamp melting apparatus and are uncorrected. Deuterated solvents for NMR purposes were obtained from Armar and used as received.

^1H and ^{13}C NMR were recorded on a Bruker Avance 400 spectrometer operating at 400 MHz (^1H) and 100 MHz (^{13}C). ^1H and ^{13}C chemical shifts were referenced internally to solvent shift (MeOD: ^1H , 3.3, ^{13}C , 49.0; acetone- d_6 : ^1H , 2.05, ^{13}C , 29.8). Chemical shifts (are quoted in ppm, the downfield direction being defined as positive. Uncertainties in chemical shifts are typically ± 0.01 ppm for ^1H and ± 0.05 for ^{13}C . Coupling constants are typically ± 0.1 Hz for ^1H - ^1H and ± 0.5 Hz for ^1H - ^{13}C couplings. The following abbreviations are used for convenience in reporting the multiplicity of NMR resonances: s, singlet; d, doublet; t, triplet; q, quartet; m, multiplet; br, broad. All NMR data was acquired and processed using standard Bruker software (Topspin).

Photophysical measurement

Emission spectra and lifetime measurements for complex **1** were performed on a PTI TimeMaster C720 Spectrometer (Nitrogen laser: pulse output 337 nm) fitted with a 380 nm filter. Error limits were estimated: λ (± 1 nm); τ ($\pm 10\%$); ϕ ($\pm 10\%$). All solvents used for the lifetime measurements were degassed using three cycles of freeze-vac-thaw.

Luminescence quantum yields were determined using the method of Demas and Crosby $^1[\text{Ru}(\text{bpy})_3][\text{PF}_6]_2$ in degassed acetonitrile as a standard reference solution ($\Phi_r = 0.062$) and calculated according to the reported equation:

$$\Phi_s = \Phi_r(B_r/B_s)(n_s/n_r)^2(D_s/D_r)$$

where the subscripts *s* and *r* refer to sample and reference standard solution respectively, *n* is the refractive index of the solvents, *D* is the integrated intensity, and Φ is the luminescence quantum yield. The quantity *B* was calculated by $B = 1 - 10^{-AL}$, where *A* is the absorbance at the excitation wavelength and *L* is the optical path length.

Luminescence response of complex 1 towards different forms of DNA

The G-quadruplex DNA-forming sequences TBA, HTS, PS2.M, Pu27 and c-kit87 were annealed in Tris-HCl buffer (20 mM Tris, 100 mM KCl, pH 7.4) and were stored at –20 °C before use. Complex 1 (1.5 μM) was added to 5 μM of ssDNA, dsDNA or G-quadruplex DNA in Tris-HCl buffer (20 mM Tris-HCl, pH 7.4), then their emission intensity were tested.

Total cell extract preparation

The TRAMPC1 (ATCC® CRL2730™) cell line was purchased from American Type Culture Collection (Manassas, VA 20108 USA). Prostate cancer cells were trypsinized and resuspended in TE buffer (10 mM Tris-HCl 7.4, 1 mM EDTA). After incubation on ice for 10 min, the lysate was centrifuged and the supernatant was collected.

Detection of lysozyme

The lysozyme aptamer-containing DNA ON1 (100 μM) and the capture DNA ON2 containing G-quadruplex-forming sequences (100 μM) were separately heated to 95 °C for 10 min. After heating, they were immediately immersed into 4 °C water to generate random-coil oligonucleotides. The DNA stock was stored at –20 °C. In the assay, 0.2 μM of ON1 was hybridized with 0.2 μM of the capture DNA ON2 through annealing at 95 °C for 10 min, cooling to room temperature at 0.1 °C/s, and further incubation at 25 °C for 1 h to confirm the formation of the dsDNA. The mixture was then reacted with various concentrations of lysozyme in 500 μL Tris-HCl buffer (20 mM Tris-HCl, 10 mM MgCl₂, 100 mM NaCl, pH 7.4) at 37 °C for 1 h. Lastly, 70 mM KCl and 1.5 μM of complex 1 were introduced into the mixture. Emission spectra were recorded in the 520–760 nm range using an excitation wavelength of 310 nm.

For the lysozyme detection in cell extract, 0.2 μM of duplex DNA ON1/ON2 was first incubated with different concentrations of lysozyme in 500 μL Tris-HCl buffer (20 mM Tris-HCl, 10 mM MgCl₂, 100 mM NaCl, pH 7.4) containing 0.5% (v/v) cell extract at

37 °C for 1 h, leading to the formation of an lysozyme-aptamer complex. The following steps are the same as described for lysozyme detection in buffered solution.

Synthesis

Complex **1** was prepared according to a (modified) literature method². Its structure was fully characterized by ¹H-NMR, ¹³C-NMR, high resolution mass spectrometry (HRMS) and elemental analysis, and its photo physical properties were also tested.

The synthesis of complex **1** is described as follows . Specifically, a suspension of [Ir₂(Br-ppy)₄Cl₂] (0.2 mmol) and 2,2'-biquinoline (0.42 mmol) in a mixture of DCM:methanol (1:1.2, 36 mL) was refluxed overnight under a nitrogen atmosphere. The resulting solution was then allowed to cool to room temperature, and filtered to remove unreacted cyclometallated dimer. Then, an aqueous solution of ammonium hexafluorophosphate (excess) was added into the filtrate, and the filtrate was reduced in volume by rotary evaporation until precipitation of the crude product occurred. The precipitate was then filtered and washed with several portions of water (2 × 50 mL) followed by diethyl ether (2 × 50 mL). The product was recrystallized in the acetonitrile:diethyl ether vapor diffusion to yield the titled compound as a red solid.

Complex **1**. Yield: 71%, ¹H NMR (400 MHz, DMSO-*d*₆) δ 9.06–8.92 (m, 4H), 8.25 (d, *J* = 7.9 Hz, 2H), 8.14 (d, *J* = 8.1, 2H), 8.01–7.89 (m, 4H), 7.83 (d, *J* = 8.5 Hz, 2H), 7.74 (d, *J* = 9.4 Hz, 2H), 7.76 (t, *J* = 8 Hz, 2H), 7.33–7.19 (m, 4H), 7.15 (t, *J* = 7.4 Hz, 2H), 6.17 (d, *J* = 2.0 Hz, 2H); ¹³C NMR (100 MHz, DMSO-*d*₆) δ 165.12, 159.76, 150.77, 150.57, 147.20, 142.41, 141.68, 139.36, 132.45, 131.14, 129.59, 129.08, 128.98, 127.10, 126.72, 125.50, 124.41, 123.63, 122.17, 120.54.; MALDI-TOF-HRMS: Calcd. for C₄₀H₂₆Br₂IrN₄ [M–PF₆]⁺: 915.0133 Found: 915.0109. Anal.: (C₄₀H₂₆Br₂F₆IrN₄P) C, H, N: calcd. 45.34, 2.47, 5.29; found 45.43, 2.67, 5.26.

Table S1. Photophysical properties of iridium(III) complex **1** in acetonitrile (298K)

Complex	Quantum yield	λ_{em}/nm	Life time/ μs	UV/vis absorption λ_{abs}/nm ($\epsilon/\text{dm}^3\text{mol}^{-1}\text{cm}^{-1}$)
1	0.195	615	4.187	271 (6.25×10^4), 371 (2.28×10^4), 485 (1.13×10^3)

Table S2. DNA sequences used in this project:

DNA	Sequence
ON1	5'- GC ₃ TC ₃ TATCAG ₃ CTA ₃ GAGTGCAGAGT ₂ ACT ₂ AGAG ₂ T ₂ G ₂ TGT G ₂ T ₂ G ₂ -3'
ON1 _b	5'- GC ₃ TC ₃ TATCAG ₃ CTA ₃ GAGTGCAGAGT ₂ ACT ₂ AGA-3'
ON2	5'- C ₂ TGATAG ₃ AG ₃ CGCTG ₃ AG ₂ AG ₃ -3'
CCR5- DEL	5'-CTCAT ₄ C ₂ ATACAT ₂ A ₃ GATAGTCAT-3'
ds17	5'-C ₂ AGT ₂ CGTAGTA ₂ C ₃ -3' 5'-G ₃ T ₂ ACTACGA ₂ CTG ₂ -3'
ds26	5'-CAATCGGATCGAATTCGATCCGATTG-3'
TBA	5'- GGTTGGTGTGGTTGG-3'
HTS	5'- GGGTTAGGGTTAGGGTTAGGG-3'
PS2.M	5'- GTGGGTAGGGCGGGTTGG-3'
Pu27	5'- TGGGGAGGGTGGGGAGGGTGGGGAAGG-3'
c-kit87	5'- AGGGAGGGCGCTGGGAGGAGGG-3'
F21T	5'-FAM-(G ₃ [T ₂ AG ₃] ₃)-TAMRA-3'
F10T	5'-FAM-TATAGCTA-HEG-TATAGCTATAT-TAMRA-3'
ON1 _m	5'- <i>GT₂CT₂CT</i> ATCAG ₃ CTA ₃ GAGTGCAGAGT ₂ ACT ₂ AGAG ₂ T ₂ G ₂ T GTG ₂ T ₂ G ₂ -3'
ON2 _m	5'- C ₂ TGATAG <i>A₂AG₂</i> CGCTG <i>A₂AG₂AG₂</i> -3'

a. The bold italic bases are mutant bases.

Table S3 Comparison of aptamer-based lysozyme detection assays reported in recent years.

Method	Selectivity	Detection limit	Reference	Labeled DNA?
Detection of lysozyme magnetic relaxation switches based on aptamer-functionalized superparamagnetic nanoparticles	Discriminate lysozyme from other protein	0.5 nM	3	No
A novel exonuclease III-aided amplification assay for lysozyme based on graphene oxide platform	Discriminate lysozyme from other biomolecules	0.08 $\mu\text{g/mL}$	4	Yes
A reagentless signal-off architecture for electrochemical aptasensor for the detection of lysozyme	Discriminate lysozyme from other biomolecules	7 nM	5	Yes
Electrochemical impedance spectroscopy detection of lysozyme based on electrodeposited gold nanoparticles	Discriminate lysozyme from other biomolecules	0.01 pM	6	No
An ultrasensitive peroxidase DNAzyme-associated aptasensor that utilizes a target-triggered	Discriminate lysozyme from other	0.1 fM	7	No

enzymatic signal amplification strategy	biomolecules			
Label-free and reagent-less protein biosensing using aptamer-modified extended-gate field-effect transistors	Discriminate lysozyme from other biomolecules	12.0 nM	8	Yes
Label-free highly sensitive detection of proteins in aqueous solutions using surface-enhanced Raman scattering	Discriminate lysozyme from other biomolecules	5 µg/mL	9	No
Sensitive colorimetric detection of lysozyme in human serum using peptide-capped gold nanoparticles	Discriminate lysozyme from other biomolecules	80 pg/mL	10	Yes
Design of ultrasensitive chemiluminescence detection of lysozyme in cancer cells based on nicking endonuclease signal amplification technology	Discriminate lysozyme from other biomolecules	0.2 pM	11	Yes
An aptamer-based biosensor for the detection of lysozyme with gold nanoparticles amplification	Discriminate lysozyme from other biomolecules	0.1 pM	12	Yes
Label-free and sensitive electrogenerated	Discriminate lysozyme from	0.12 nM	13	No

chemiluminescence aptasensor for the determination of lysozyme	other biomolecules			
Lysozyme aptamer biosensor based on electron transfer from SWCNTs to SPQC-IDE	Discriminate lysozyme from other biomolecules	0.5 nM	14	Yes
A sensitive, non-damaging electrochemiluminescent aptasensor via a low potential approach at DNA-modified gold electrodes	Discriminate lysozyme from other biomolecules	0.45 pM	15	No
Label-free and sensitive faradic impedance aptasensor for the determination of lysozyme based on target-induced aptamer displacement	Discriminate lysozyme from other biomolecules	0.07 nM	16	Yes
Enhancing the Sensitivity of Aptameric Detection of Lysozyme with a “Feed-Forward” Network of DNA-Related Reaction Cycles	Discriminate lysozyme from other biomolecules	3.6 fM	17	Yes
Label-free electrochemical aptasensor for the detection of lysozyme	Discriminate lysozyme from other biomolecules	36.0 nM (if considerin g guanine signal) and	18	No

		18.0 nM (if taking adenine oxidation current).		
Lysozyme detection on aptamer functionalized graphene-coated SPR interfaces	Discriminate lysozyme from other biomolecules	0.5 nM	19	No
Fluorescence turn-on detection of a protein through the displaced single-stranded DNA binding protein binding to a molecular beacon	Discriminate lysozyme from other biomolecules	200 pM	20	No
Graphene-based lysozyme binding aptamer nanocomposite for label- free and sensitive lysozyme sensing	Discriminate lysozyme from other biomolecules	6 fM	21	No

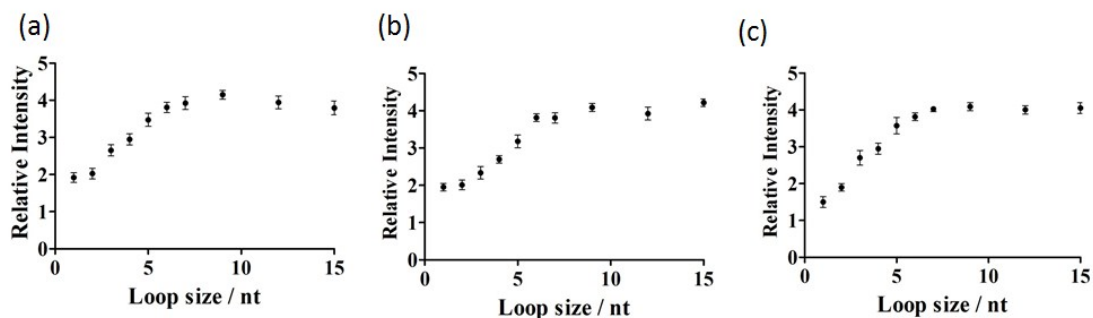


Fig. S1. (a) Luminescence enhancement of complex **1** ($1 \mu\text{M}$) as a function of 5'-side loop, $5'-\text{G}_3\text{T}_n\text{G}_3\text{T}_3\text{G}_3\text{T}_3\text{G}_3-3'$. (b) Luminescence enhancement of complex **1** ($1 \mu\text{M}$) as a function of central loop, $5'-\text{G}_3\text{T}_3\text{G}_3\text{T}_n\text{G}_3\text{T}_3\text{G}_3-3'$ and (c) Luminescence enhancement of complex **1** ($1 \mu\text{M}$) as a function of 3'-side loop, $5'-\text{G}_3\text{T}_3\text{G}_3\text{T}_3\text{G}_3\text{T}_n\text{G}_3-3'$ (in nucleotides).

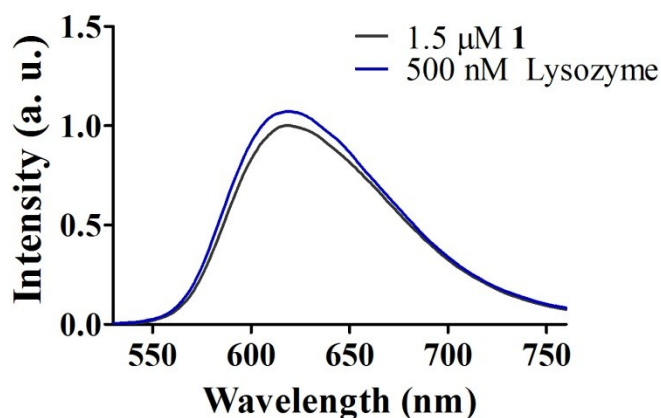


Fig. S2. Luminescence response of the system with the complex alone ($[\text{complex } \mathbf{1}] = 1.5 \mu\text{M}$) in the absence and presence of lysozyme (500 nM).

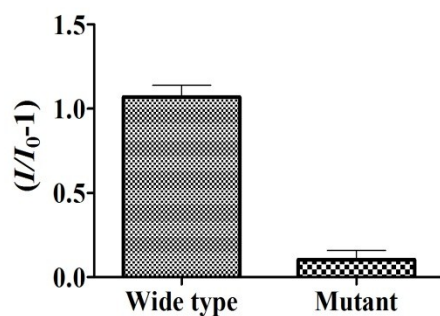


Fig. S3. Relative luminescence responses of complex **1** (1.5 μM) in the system containing wild-type or mutant DNA. Error bars represent the standard deviations of the results from three independent experiments.

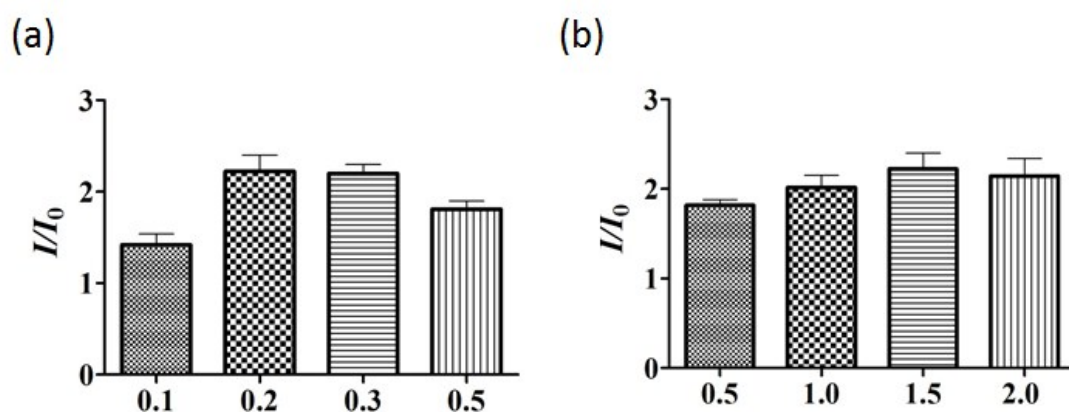


Fig. S4. (a) Relative luminescence response of the system in the absence or presence of lysozyme (50 nM) at various concentrations of ON1/ON2 (0.1, 0.2, 0.3 and 0.5 μM). (b) Relative luminescence response of the system in the absence or presence of lysozyme (50 nM) at various concentrations of complex **1** (0.5, 1.0, 1.5 and 2.0 μM). Error bars represent the standard deviations of the results from three independent experiments.

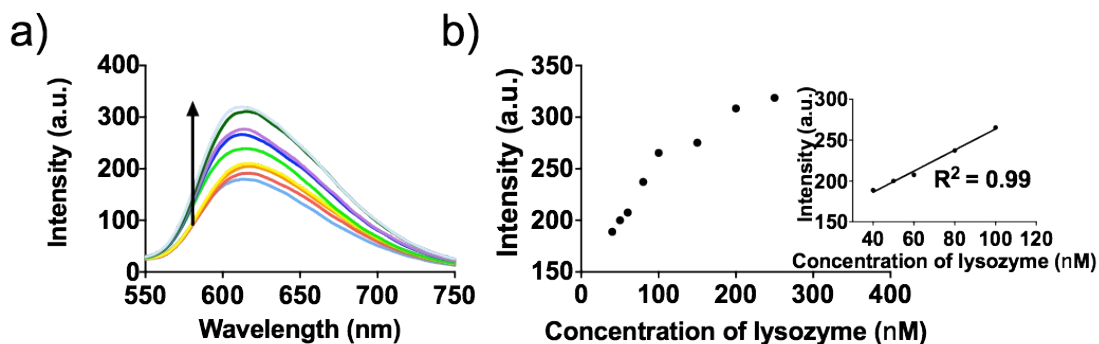


Fig. S5 (a) Luminescence spectra of the 1/ON1_b/ON2 system in response to various concentrations of lysozyme: 0, 40, 50, 60, 80, 100, 150, 200 and 250 nM. (b) The relationship between luminescence intensity at $\lambda = 615$ nm and lysozyme concentration. Inset: linear plot of the change in luminescence intensity at $\lambda = 615$ nm vs. lysozyme concentration.

Reference

1. G. A. Crosby and J. N. Demas, *J. Phys. Chem.*, 1971, **75**, 991-1024.
2. Q. Zhao, T. Cao, F. Li, X. Li, H. Jing, T. Yi and C. Huang, *Organometallics*, 2007, **26**, 2077-2081.
3. S. Bamrungsap, M. I. Shukoor, T. Chen, K. Sefah and W. Tan, *Anal. Chem.*, 2011, **83**, 7795-7799.
4. C. Chen, J. Zhao, J. Jiang and R. Yu, *Talanta*, 2012, **101**, 357-361.
5. Z. Chen and J. Guo, *Electrochim. Acta*, 2013, **111**, 916-920.
6. Z. Chen, L. Li, H. Zhao, L. Guo and X. Mu, *Talanta*, 2011, **83**, 1501-1506.
7. R. Fu, K. Jeon, C. Jung and H. G. Park, *Chem. Commun.*, 2011, **47**, 9876-9878.
8. T. Goda and Y. Miyahara, *Biosens. Bioelectron.*, 2013, **45**, 89-94.
9. X. X. Han, G. G. Huang, B. Zhao and Y. Ozaki, *Anal. Chem.*, 2009, **81**, 3329-3333.
10. H. Huang, Q. Zhang, J. Luo and Y. Zhao, *Anal. Methods*, 2012, **4**, 3874-3878.
11. X. Hun, H. Chen and W. Wang, *Biosens. Bioelectron.*, 2010, **26**, 248-254.
12. L.-D. Li, Z.-B. Chen, H.-T. Zhao, L. Guo and X. Mu, *Sensor Actua B-Chem*, 2010, **149**, 110-115.
13. Y. Li, H. Qi, Q. Gao and C. Zhang, *Biosens. Bioelectron.*, 2011, **26**, 2733-2736.
14. Y. Lian, F. He, X. Mi, F. Tong and X. Shi, *Sensor Actuat. B-Chem.*, 2014, **199**, 377-383.
15. D.-Y. Liu, Y.-Y. Xin, X.-W. He and X.-B. Yin, *Analyst*, 2011, **136**, 479-485.
16. Y. Peng, D. Zhang, Y. Li, H. Qi, Q. Gao and C. Zhang, *Biosens. Bioelectron.*, 2009, **25**, 94-99.
17. R. Ren, Z. Yu, Y. Zou and S. Zhang, *Chem. Eur. J.*, 2012, **18**, 14201-14209.
18. M. C. Rodríguez and G. A. Rivas, *Talanta*, 2009, **78**, 212-216.

19. P. Subramanian, A. Lesniewski, I. Kaminska, A. Vlandas, A. Vasilescu, J. Niedziolka-Jonsson, E. Pichonat, H. Happy, R. Boukherroub and S. Szunerits, *Biosens. Bioelectron.*, 2013, **50**, 239-243.
20. D. Tang, D. Liao, Q. Zhu, F. Wang, H. Jiao, Y. Zhang and C. Yu, *Chem. Commun.*, 2011, **47**, 5485-5487.
21. Y. Xiao, Y. Wang, M. Wu, X. Ma and X. Yang, *J. Electroanal. Chem.*, 2013, **702**, 49-55.